nature immunology

Sphingosine 1-phosphate type 1 receptor agonism inhibits transendothelial migration of medullary T cells to lymphatic sinuses

Sindy H Wei[1,5], Hugh Rosen[2,5], Melanie P Matheu[1], M Germana Sanna[2], Sheng-Kai Wang[3], Euijung Jo[2], Chi-Huey Wong[3], Ian Parker[4], & Michael D Cahalan[1]

Sphingosine 1-phosphate type 1 ($S1P_1$) receptor agonists cause sequestration of lymphocytes in secondary lymphoid organs by a mechanism that is not well understood. One hypothesis proposes that agonists act as 'functional antagonists' by binding and internalizing $S1P_1$ receptors on lymphocytes; a second hypothesis proposes instead that $S1P_1$ agonists act on endothelial cells to prevent lymphocyte egress from lymph nodes. Here, two-photon imaging of living T cells in explanted lymph nodes after treatment with $S1P_1$ agonists or antagonists has provided insight into the mechanism by which $S1P_1$ agonists function. The selective $S1P_1$ agonist SEW2871 caused reversible slowing and 'log-jamming' of T cells between filled medullary cords and empty sinuses, whereas motility was unaltered in diffuse cortex. Removal or antagonist competition of SEW2871 permitted recovery of T cell motility in the parenchyma of the medulla and resumption of migration across the stromal endothelial barrier, leading to refilling of sinuses. Our results provide visualization of transendothelial migration of T cells into lymphatic sinuses and suggest that $S1P_1$ agonists act mainly on endothelial cell $S1P_1$ receptors to inhibit lymphocyte migration.

FTY720 is a reversible immunosuppressive agent, now in human clinical trials for renal transplantation, that prevents graft rejection and the development of autoimmunity in experimental animal models[1]. The phosphorylated form of FTY720 binds to G protein–coupled sphingosine 1-phosphate type 1 receptors ($S1P_1$ receptors) on target cells and induces lymphopenia by sequestering lymphocytes inside lymphoid organs[2,3]. In the presence of the phosphorylated form of FTY720 analogs and other $S1P_1$ receptor agonists, the medullary and subcapsular sinuses of lymph nodes become cleared of lymphocytes, whereas lymphocytes become heavily packed and queued up ('log-jammed') against the sinus endothelium[2,4].

The mechanisms underlying this effect remain controversial, and two alternative hypotheses have been proposed involving different loci of action of $S1P_1$ ligands. One hypothesis, referred to as 'functional antagonism'[5], states that some agonists such as the phosphorylated form of FTY720 bind directly to $S1P_1$ receptors on lymphocytes themselves and cause receptor internalization and degradation, which in turn prevents lymphocyte migration from the lymph node dependent on chemotaxis along a gradient of endogenous S1P. In support of that hypothesis, lymphocytes pretreated with FTY720 (ref. 5) show reduced $S1P_1$ receptor expression and chemotaxis *in vitro*, and lymphocytes from $S1P_1$-deficient mice fail to egress from thymus, spleen and lymph node[5,6]. The second hypothesis states that ligand binding to $S1P_1$ receptors on endothelial cells results in 'downstream' signaling events and changes in endothelial cytoskeletal organization that alter barrier function, which thereby blocks lymphocyte egress from the medullary parenchyma into draining sinuses[2]. According to the second hypothesis, $S1P_1$ receptor agonism on endothelial cells, not in lymphocytes themselves, serves a 'gatekeeper' function by sequestering lymphocytes in the lymph node.

One method to distinguish between the hypotheses described above is with imaging studies in intact, three-dimensional, secondary lymphoid environments. This method is especially important because many studies have been limited to providing 'snapshots' of fixed tissue specimens that provide no information of cell dynamics[2,3,5–7]. Intravital imaging[8] has confirmed the high T cell velocities and 'random walk' motility patterns seen originally in the cortex of lymph node explants[9]. We thus applied real-time two-photon microscopy to visualize motility and transendothelial migration of individual T cells into lymphatic sinuses in intact, explanted lymph nodes. Such imaging techniques have been used to characterize trafficking of T lymphocytes and B lymphocytes in the cortical and follicular regions of the lymph node[9], and by simply inverting the node on the microscope stage, we were able to visualize lymphocyte motility and distribution in medullary regions. These studies were facilitated by the use of a reversible, high-affinity $S1P_1$ receptor agonist, SEW2871, and

[1]Department of Physiology and Biophysics and Center for Immunology, University of California, Irvine, California 92697-4561, USA. [2]Department of Immunology and [3]Department of Chemistry, The Scripps Research Institute, La Jolla, California 92037, USA. [4]Department of Neurobiology and Behavior, University of California, Irvine, California 92697-4550, USA. [5]These authors contributed equally to this work. Correspondence should be addressed to M.D.C. (mcahalan@uci.edu) or H.R. (hrosen@scripps.edu).

Received 30 June; accepted 16 September; published online 6 November 2005; doi:10.1038/ni1269

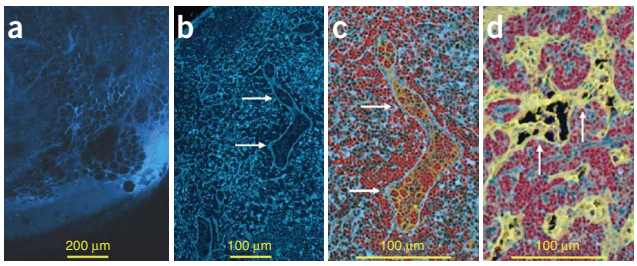

Figure 1 Delineation of structures in control or SEW2871-treated lymph nodes by a fluorescent lectin that overlaps with LYVE-1 staining. (**a**) Confocal image of a section obtained after incubation of an intact inguinal node at 4 °C with Alexa Fluor 633–conjugated WGA. (**b**) Confocal immunofluorescence image of a fixed inguinal node section from a vehicle-treated C57BL/6 mouse, stained with WGA (blue 'pseudocolor'). Arrows indicate staining of lymphatic sinus by WGA. (**c**) Confocal triple-immunofluorescence image of a fixed inguinal node section (enlarged view of area shown in **b**) from a vehicle-treated C57BL/6 mouse stained with LYVE-1 rabbit polyclonal antibody to mouse (yellow), antibody to B220 (red) and WGA (blue). LYVE-1 antibody staining outlines lymphatic sinuses surrounded by a WGA^+ basement membrane (arrows), with $B220^+$ lymphocytes in both the medullary cord and in the lumen of the lymphatic sinuses. (**d**) Image obtained from an SEW2871-treated mouse and stained as described in **c**. LYVE-1 expression is upregulated and sinuses (arrows) are emptied of lymphocytes.

two receptor antagonists, W123 and VPC23019. SEW2871 is a selective agonist for $S1P_1$, with a 50% effective concentration of 10–20 nM on mouse and human receptors[3]. Because it overlaps with the endogenous S1P binding site[10], SEW2871 can activate all known signals downstream of the receptor. In addition, like endogenous S1P (but in contrast to the agonist, phosphorylated FTY720) SEW2871 induces receptor internalization and recycling but not receptor degradation[10]. Furthermore, long-term *in vivo* treatment of mice with SEW2871 induces and maintains inhibition of egress from thymus and lymph nodes, which leads to the clearing of both cortical and medullary lymphatic sinuses of lymphocytes. This sequestration is reversed with kinetics inversely proportional to the plasma concentration of SEW2871 (ref. 3). W123 (S.-K.W., C.-H.W., M.G.S. and H.R., unpublished data) and VPC23019 (ref. 11) are analogs of FTY720 that are competitive antagonists of $S1P_1$ receptor activation by SEW2871, as measured by GTPγS activation, mitogen-activated protein kinase recruitment, cell migration and ligand-induced receptor internalization.

We show here that the $S1P_1$ receptor agonist SEW2871 specifically reduced lymphocyte velocity and motility in the medullary region but not the diffuse cortex of the lymph node. Inhibition by SEW2871 of lymphocyte motility and transmigration across the lymphatic endothelium was rapidly reversed by removal ('washout') of the agonist or by the addition of antagonist in the continuous presence of agonist. These results are consistent with a mechanism whereby continuous $S1P_1$ agonist signals on endothelial cells – not on lymphocytes themselves – are required for medullary arrest of lymphocytes. These studies demonstrate the dynamic aspects of transendothelial migration of T cells into the lymphatic sinus, an important step in egress control of T cells leaving the lymph node.

RESULTS

Imaging transendothelial migration into the lymphatic sinus

A crucial step in the egress of lymphocytes from the lymph node involves their migration from medullary cords into the sinus spaces leading to efferent lymphatic vessels. To image that process, we oriented excised lymph nodes with the hilum facing the objective lens so that the medullary region lay sufficiently close to the surface of the node to be visualized (**Supplementary Fig. 1** online). We also developed methods to identify the microanatomic sites where lymphocytes encounter stromal barriers, such as the lymphatic endothelium, that are involved in the control of egress. We found that incubating the explant with a fluorescent wheat germ agglutinin (WGA) efficaciously labeled medullary sinus structures at imaging depths between 40 and 80 μm (**Fig. 1a**). Moreover, WGA stained a stromal component immediately subjacent to the antibody LYVE-1 staining of hyaluronan receptors on lymphatic (but not vascular) endothelium (**Fig. 1b–d**), demonstrating that WGA highlights the walls of medullary sinuses but does not label lymphocytes. Furthermore, the accumulation of lymphocytes surrounding empty sinus spaces induced by the $S1P_1$-selective agonist SEW2871 also provided a confirmatory landmark. Control nodes showed a more uniform distribution of lymphocytes between medullary tissue and sinuses (**Fig. 1c**), whereas nodes treated with SEW2871 showed lymphocytes log-jammed around the sinus-lining endothelium, with sinuses notably void of lymphocytes (**Fig. 1d**). These images also demonstrated increased LYVE-1 staining after SEW2871 treatment, probably reflecting a structural or functional rearrangement in lymphatic endothelium.

Reversible agonist inhibition of T cell motility and migration

WGA staining provided an important landmark to guide our two-photon imaging experiments of living T cells interacting with and migrating across the lymphatic endothelium into the sinus. We obtained an image of a two-photon '*z*-slice' (82 μm × 100 μm × 10 μm) in the medullary region of an intact, explanted node from a mouse gavaged with SEW2871 (**Fig. 2a**). We identified a sinus space both as a weakly stained area in the WGA image channel and as a region almost entirely devoid of labeled T cells but surrounded by many labeled cells in the adjacent tissue. In contrast, nodes that were never exposed to SEW2871 had T cells present at roughly equal numbers in both the sinus spaces and surrounding tissue (**Fig. 2b**). We confirmed T cell localization in three-dimensional space by volumetric rendering of these lymphatic sinuses (**Supplementary Video 1** online). Moreover, whereas T cells in SEW2871-treated nodes generally showed a rounded morphology before washout ('shape index', determined by dividing the long diameter by the short diameter, 1.36 ± 0.04; $n = 75$), those in control nodes or after SEW2871 washout were more polarized (shape index, 1.89 ± 0.07; $n = 60$).

To examine the effects of SEW2871 on lymphocyte motility and migration into the lymphatic sinus, we superimposed sequential 'snapshots' (as in **Fig. 2a**) over 5.8-minute time intervals to create composite images in which T cells 'traced out' their own tracks (**Fig. 2c**) and plotted the tracks of randomly selected T cells normalized to their respective starting positions (**Fig. 2d**). In the presence of SEW2871, motility was strongly hindered and cells generally moved less than 10 μm throughout each 5.8-minute period (**Fig. 2c,d**, top). After washout of the drug, T cell motility progressively recovered over about 30 min, and cells migrated into the sinus spaces (**Fig. 2c,d**, middle and bottom, and **Supplementary Videos 1** and **2** online). By comparison, control nodes without exposure to SEW2871 showed vigorous T cell motility in which lymphocyte localization and displacement from the origin did not change appreciably over comparable time periods (**Fig. 2e,f** and **Supplementary Video 3** online).

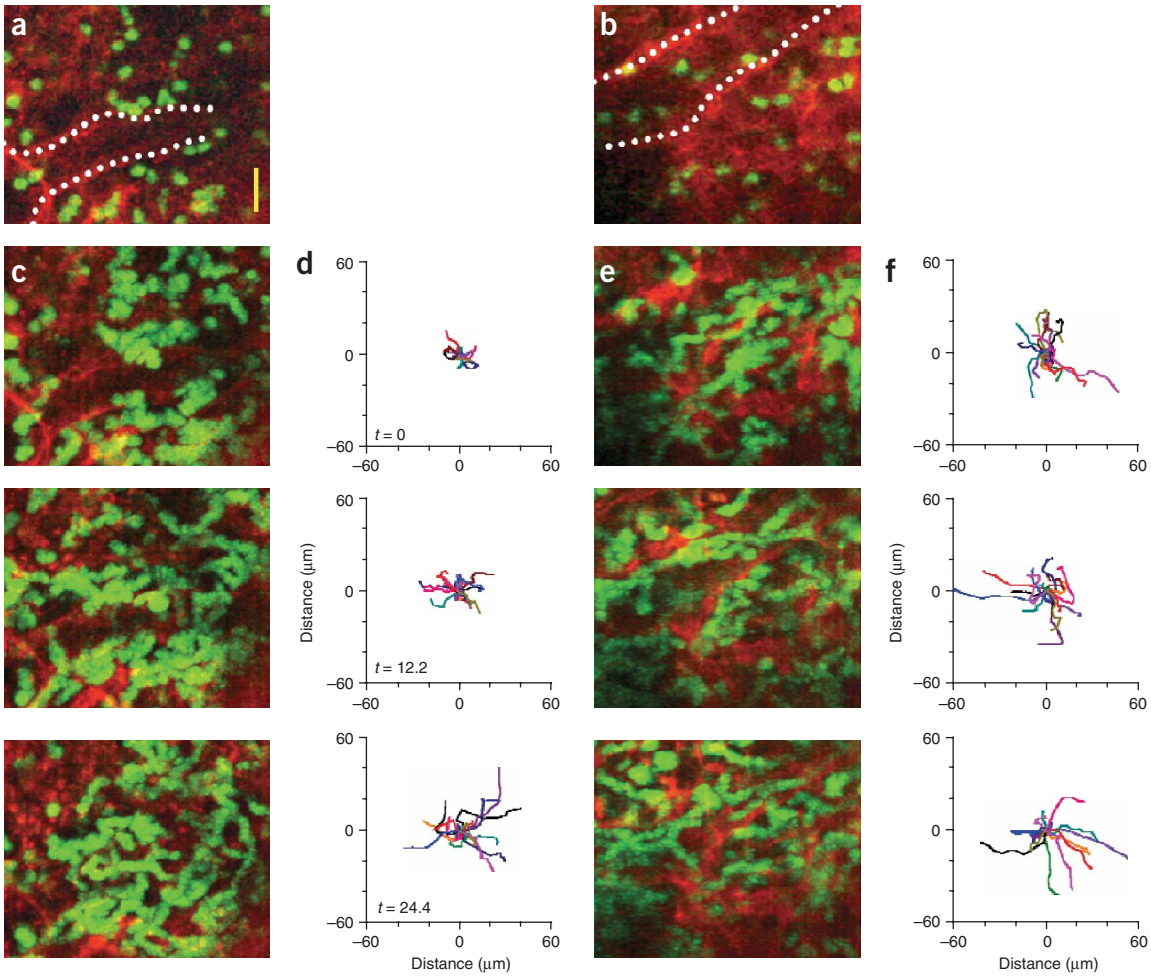

Figure 2 Motility and transendothelial migration of T cells are inhibited by SEW2781 but rapidly recover after drug washout. (**a**) Two-photon image of a medullary region of a lymph node from a mouse treated with SEW2871, presented as a maximum intensity projection through a 10-μm axial depth, showing adoptively transferred T cells labeled with 5-(and-6)-carboxyfluorescein diacetate, succinimidyl ester (green) and tissue stained with Alexa Fluor 633–WGA (red). White dots outline a sinus boundary. Scale bar, 20 μm. (**b**) Image corresponding to that in **a**, obtained in a control node in the absence of SEW2871. (**c**) Changes in T cell distribution and motility during washout of SEW2871. Each image was formed by the summation of successive images (**Supplementary Video 2** online) over a 5.8-minute period, so that T cells effectively 'trace out' their own tracks. Images were acquired (top to bottom) approximately 5 min after placement of the node in SEW2871-free superfusate to allow for temperature equilibration ($t = 0$) and then at later times ($t = 12.2$ and $t = 24.4$ min). (**d**) Lateral (x-y) tracks of 20 T cells, monitored throughout 4-minute periods beginning at times corresponding to the images in **c** and normalized to starting coordinates. (**e**,**f**) Images and T cell tracks obtained in control conditions at the same time intervals in **c**,**d** (**Supplementary Video 3** online). This node was from a mouse gavaged with vehicle only, and SEW2871 was omitted from the superfusion solution. Representative of a total of four SEW2871-treated and two vehicle-treated nodes imaged using similar conditions.

Region-specific effects of SEW2871 on T cell velocity

We determined the effects of SEW2871 on instantaneous T cell velocities in different regions of the node (**Fig. 3** and **Table 1**). T cell velocities in the medulla of control nodes averaged about 6 μm/min, but slowed to less than one half that value over 10–30 min after the addition of 5 μM SEW2871 to the bathing medium (**Fig. 3a**). Washout of SEW2871 resulted in full recovery of motility with a similar time course (**Fig. 3b**,**c**). Thus, the arrest was not an artifact of photodamage resulting from continued laser irradiation, a conclusion also supported by the consistency noted in T cell velocities throughout 30-minute imaging periods in the absence of SEW2871 (**Fig. 3d**). In notable contrast to the action of SEW2871 in slowing T cells in medullary tissue, cells in the T cell zone were unaffected by the drug (**Fig. 3e** and **Supplementary Video 4** online), with high velocities (11–12 μm/min) similar to those in control conditions in both explanted and *in vivo* lymph nodes[8,9], regardless of whether SEW2871 was present.

To further characterize the motility of T cells, we constructed mean displacement plots by graphing the absolute distances of cells from their starting points during six successive 5.8-minute time frames (**Fig. 3c–e**). Consistent with a 'random walk' motion[9], the mean T cell displacements increased proportional to the square root of time for all experimental conditions (**Fig. 3f–h**). The slope of this relationship yielded a two-dimensional 'motility coefficient', equal to x^2 divided by $4t$, where 'x' is the mean distance from the origin at time 't'. SEW2871 considerably decreased the motility coefficient of T cells in the medulla, but motility recovered after washout of the drug (**Fig. 3f**). However, even in the absence of any exposure to SEW2871, the motility coefficient in the medulla (**Fig. 3g**) was appreciably smaller than that in the cortical T cell zone (**Table 1**). SEW2871 did

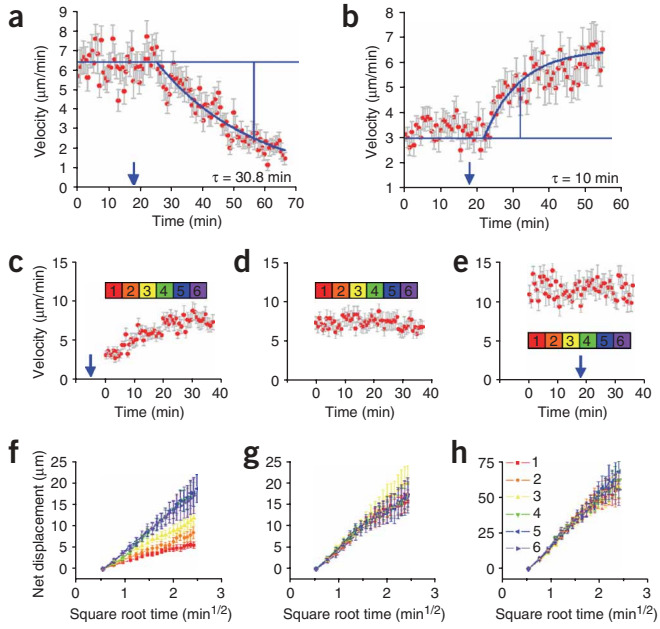

Figure 3 Selective and reversible inhibition of T cell motility in the medulla. (**a**) Decrease in T cell velocities in the medulla of an axillary node from a vehicle-treated mouse after superfusion with 5 μM SEW2871 (downward arrow). Fitted curve is an exponential with a time constant (τ) of 30.8 min. (**b**) Decreased velocity in the medulla of an axillary node from an SEW2871-treated mouse during superfusion with 5 μM SEW2871, and recovery after agonist washout (downward arrow). τ = 10 min. (**c**) Recovery of T cell velocity in the medulla after washout of SEW2871 (downward arrow) in another node (**Supplementary Video 2** online). (**d**) Control experiment showing time-invariant velocity of T cells in the medulla of a node never exposed to SEW2871 (**Supplementary Video 3** online). (**e**) Velocity of T cells in the T cell zone of the cortex is unaffected by SEW2871 (**Supplementary Video 4** online). Node is from an SEW2871-treated mouse, with subsequent washout of drug (downward arrow). (**f–h**) Plots of mean displacement of T cells versus square root of time, derived from the corresponding experiment (**c–e**) above each graph. Data were obtained by measurement of the mean absolute displacement of T cells from their starting positions over consecutive 5.8-minute epochs, indicated by colors corresponding to the time periods (1–6) marked in **c–e**. Data points show mean ± 1 s.e.m. of measured instantaneous velocities.

not appreciably alter motility coefficients in the T cell zone (**Fig. 3h** and **Table 1**), emphasizing the microanatomic specificity of the SEW2871 effect on motility and displacement.

Directionality of T cell migration

Although T cell trajectories (**Fig. 2**) showed changes in motility after washout of SEW2871, these data did not provide information regarding the direction of motion. To help depict the orientation of cell movements in relation to the sinus boundary, we rotated visualized tracks of T cells so that the walls of the adjacent sinus boundary aligned with the horizontal axis (**Fig. 4a,b**). Thus oriented, T cells in the vicinity of the sinus showed strongly anisotropic activity in the presence of SEW2871 (**Fig. 4a**). Few or no cells migrated into the sinus space; instead, T cells moved laterally along the sinus boundary and away from the boundary into the medullary tissue. Notably, this anisotropic movement was reversible after washout SEW2871 for 30 min, after which T cells followed random paths (**Fig. 4b**).

We tracked the resulting redistribution of cells from medullary tissue to sinus by counting T cells in defined volumes of the sinus and adjacent medulla at various times after initiating washout of SEW2871 (**Fig. 4c,d**). Initially, labeled T cells were present at only low density in the sinus, but their numbers subsequently increased toward an equilibrium over 20–30 min (**Fig. 4e**, red trace). At the same time, the number of cells in the medullary tissue decreased to a density similar to that in the sinus (**Fig. 4e**, blue trace). Nodes without exposure to SEW2871 showed roughly equivalent, time-invariant cell densities in both the sinus and medulla (**Fig. 4f**). In some instances we noted linearly directed motion of T cells in a sinus, very different from the 'random walk' trajectories in medullary tissue (**Fig. 4b**) or the T cell zone[9]. T cells traveled in a uniform direction constrained by the sinus boundaries at roughly constant velocities of 3.9 μm/min, seeming to be moving under the influence of a bulk flow rather than as autonomous individual cells (**Fig. 4g,h** and **Supplementary Video 5** online).

Physical barrier to transendothelial migration

Inhibition of T cell transendothelial migration by SEW2871 seemed to be mediated by a physical barrier in the medullary region. Specifically, we noted motile T cells that pushed repeatedly and unsuccessfully against sinus boundaries while in the presence of SEW2871. In contrast, soon after washout of SEW1871 began, T cells began to traverse the stromal endothelial barrier (**Fig. 5a** and **Supplementary Video 6** online). T cells that were initially log-jammed on the side of the sinus cavity away from the lumen regained their polarity and rapidly (within 2–3 min) moved through the endothelial tissue and came to rest in the lumen (**Fig. 5**). After washout of SEW2871, the movement of T cells across the stromal barrier was initially unidirectional, probably because the sinuses were devoid of T cells. However, in control conditions, T cells traversed in both directions across the lymphatic endothelium (**Fig. 5b** and **Supplementary Video 7** online). Notably, cells crossed between medullary cord and sinus more frequently at certain sites, which we interpreted to be stromal 'gates', or sites at which migration is possible and regulated (**Fig. 5c** and **Supplementary Video 8** online). These data are consistent with the hypothesis that $S1P_1$ receptor agonism is required for the stimulated inhibition of an egress process that is constitutive and unregulated in physiological conditions[2].

$S1P_1$ antagonists restore T cell migration and velocity

As an independent means of evaluating the function of $S1P_1$ receptor agonist activity, we used two different $S1P_1$-selective competitive antagonists, W123 and VPC23019, to determine if lymphocyte

Table 1 Region-specific effects of SEW2871

	Control	Control	SEW2871	SEW2871
	Velocity	Motility coefficient	Velocity	Motility coefficient
Medulla	6.6 ± 0.1 n = 6,915	20.6	3.4 ± 0.1 n = 3,381	1.8
Cortex	11.7 ± 0.3 n = 1,884	299	11.2 ± 0.2 n = 2,619	296

Measurements are of the cortical T cell zone and the medulla of peripheral lymph nodes either treated with vehicle (control) or exposed to SEW2871 by gavage of the mouse followed by continued superfusion with SEW2871. Instantaneous velocities (μm/min) are calculated from the mean distance traveled between successive images; n = number of measurements. Two-dimensional motility coefficients (μm^2/min) are derived from the slope of plots of mean displacement from origin versus square root of time in thin 10-μm sections (**Fig. 3f–h**).

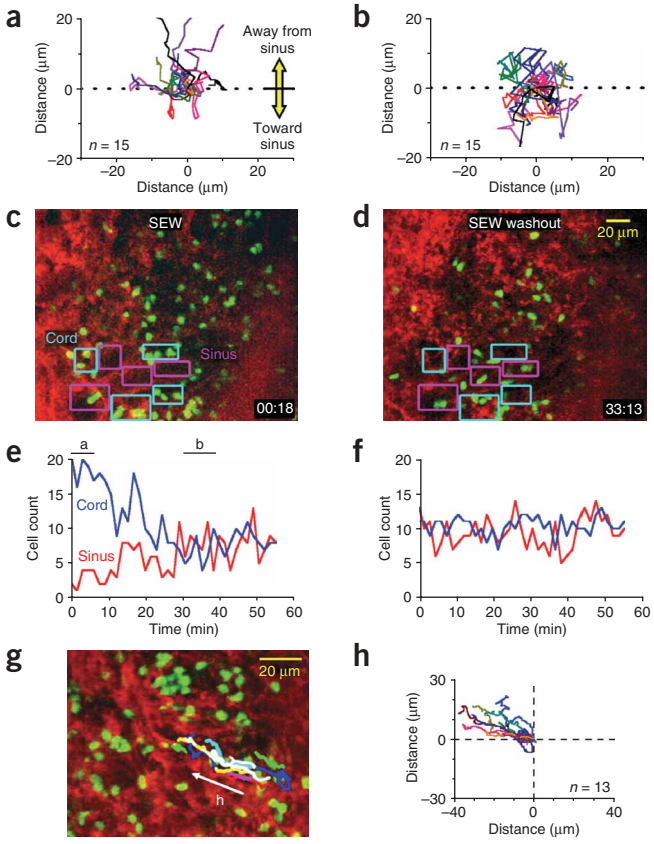

Figure 4 Directionality of T cell movement. (**a**) SEW2871 prevents T cells from crossing into sinus. Trajectories (4 min in duration) of cells near sinus boundaries were normalized to their origins and are plotted with respect to sinus wall (dotted line). Data were obtained immediately after perfusion of medium but before the drug could have washed out from tissue. (**b**) Trajectories in the same field as in **a**, tracked more than 30 min after SEW2871 washout. (**c**) Maximum intensity projection through a 10-μm axial depth of medulla imaged immediately after removal of SEW2871 (SEW) from superfusate. Boxes indicate comparable volumes in sinuses (magenta) and adjacent cords (cyan), defined by WGA staining, used to determine cell numbers plotted in **e**. (**d**) Image corresponding to **c**, obtained more than 30 min after washout, showing redistribution of T cells between sinus and cords measured in **f**. Acquisition times in **c**,**d** are indicated in minutes:seconds. (**e**) Number of labeled T cells in sinus (red) and cord (blue) in the volumes outlined in **c**,**d**. Data were obtained from the experiment in **a**,**b**; bars above graphs indicate the times during which cells were tracked. (**f**) T cell numbers corresponding to the graph in **e** in a control node without exposure to SEW2871, showing no time-dependent changes. (**g**,**h**) Passive bulk flow of T cells in a medullary sinus. (**g**) 'Snapshot' of a control node (**Supplementary Video 5** online) overlaid by trajectories of T cells in the sinus over an 18-minute period. (**h**) T cell tracks corresponding to the image in **g**.

sequestration by SEW2871 involves $S1P_1$ agonism or antagonism. As before, nodes obtained from SEW2871-gavaged mice and superfused with SEW2871 during imaging demonstrated reversible clearance of sinus spaces and a sustained decrease in T cell motility in the medullary tissue (**Fig. 6a–d**). This was reversed after the addition of W123 to the medium, even in the continued presence of SEW2871 (**Supplementary Video 9** online). The motility of T cells resumed (**Fig. 6d**) with kinetics (time constant, 14–17 min) similar to those noted after washout of SEW2871. Notably, the addition of W123 alone had no effect on T cell velocities in either medulla or cortex (**Fig. 6e**,**f**). A second $S1P_1$ receptor antagonist, VPC23019 (ref. 11), also reversed the actions of the agonist: T cell velocities increased from 4.1 ± 0.1 μm/min ($n = 100$ cells) in the presence of SEW2871 alone to 8.4 ± 0.2 μm/min ($n = 100$ cells) 30 min after the addition of VPC23019 in the presence of SEW2871. Thus, data showing that two independent and structurally distinct competitive antagonists reversed the effects of $S1P_1$-selective receptor agonism further demonstrated that continuous signaling through the receptor is required for the maintenance of lymphocyte sequestration (**Supplementary Fig. 2** online).

DISCUSSION

The study of lymphocyte egress from medullary cords into lymphatic sinuses has received considerable attention prompted by a growing appreciation that this process, apparently unregulated during constitutive lymphocyte recirculation, is subject to strong and rapid regulation by immunosuppressants acting on $S1P_1$ receptors[2,3]. Here we have described imaging of lymphocyte migration from the matrix of the lymph node into medullary sinuses and have provided new mechanistic insights regarding this process and its pharmacological regulation by $S1P_1$ agonists and antagonists. Using two-photon imaging of the hilum of explanted lymph nodes, we were able to visualize T cell dynamics in the medullary region, which is otherwise difficult to access and define structurally in intravital preparations[12]. Despite the disruption of blood and lymphatic circulation, T cells exited from medullary cords into lymphatic sinuses, indicating that the explanted node provides a readily accessible preparation in which to study transendothelial migration of lymphocytes. Moreover, pharmacological agents could be rapidly applied and washed out from the explant without the pharmacokinetic hurdle of long plasma half-lives in mice. To further capitalize on these advantages, we devised an effective means to stain stromal tissue with fluorescence-labeled WGA.

Lymph nodes treated with the reversible $S1P_1$ agonist SEW2871 (ref. 10) showed T lymphocytes log-jammed along the borders of medullary sinuses that were devoid of T cells, confirming findings in fixed tissue sections using both this agent and the related immunosuppressant FTY720 (refs. 2,3). More notably, live-cell imaging showed that such log-jamming of T cells was characterized by a discrete directional alteration in lymphocyte activity and not by complete arrest. Specifically, T cells were able to move in medullary cords and along sinus boundaries but were unable to traverse into lymphatic sinuses, suggesting that $S1P_1$ agonists negatively modulate the physical crossing of the sinus boundary into efferent lymphatics. Although T cell motility was slowed by SEW2871, this effect was specific to cells in the medulla, as T cell velocities in cortical areas were unaffected. The effects of SEW2871 were rapidly reversed with washout or by the addition of two distinct S1P1 antagonists in the continued presence of SEW2871, leading to refilling of sinuses.

These results elucidate two chief, related issues concerning the mechanism by which $S1P_1$ agonists induce lymphopenia: what are their actions on $S1P_1$ receptors and on what cells do they act. It has been proposed that immunosuppressants such as FTY720 exert a functional antagonism, whereby binding to $S1P_1$ receptors on lymphocytes promotes receptor downregulation, which in turn prevents their chemotaxis from the lymph node toward endogenous S1P in lymph[13]. However, many findings presented here provide evidence against that interpretation.

We noted a rapid (10–30 min) onset and recovery of T cell motility and transendothelial migration after application and washout of SEW2871, consistent with finding that lymphocyte entry into thoracic

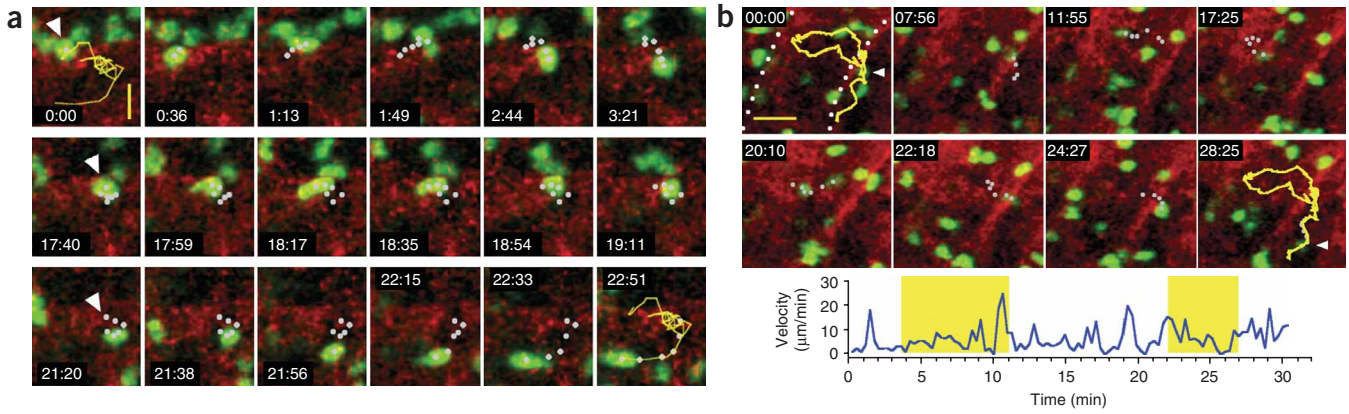

Figure 5 Imaging of lymphocyte migration across the stromal barrier. (**a**) Image sequence (from **Supplementary Video 6** online) showing a single T cell (arrowheads, far left column) traversing the stromal endothelial barrier (red; Alexa Fluor 633–WGA staining) during washout of SEW2871. Times of image acquisition are indicated in minutes:seconds; the cumulative T cell track throughout the imaging period is in yellow in the first and last panels. Grey dots ('tails') indicate the positions of the cell during the presented and several preceding frames. Scale bar, 10 μm. (**b**) Bidirectional motion of a T cell across a sinus boundary. Image sequence (from **Supplementary Video 7** online) shows the motion of a single T cell (arrowheads, first and last frames) in a control lymph node without exposure to SEW2871. Sinus boundaries are outlined in white dots in the first panel; yellow traces in the first and last panels indicate the entire trajectory of the cell. Grey dots trace the immediate 'tail' of the cell, as in **a**. Scale bar, 20 μm. Bottom, instantaneous velocity of this cell; yellow areas correspond to times when the cell traversed the sinus wall. (**c**) Multiple T cells cross the sinus boundary at a common stromal 'portal' (from **Supplementary Video 8** online). Left, trajectories of five cells overlaid on a snapshot of the sinus and surrounding medullary region (red; stained with Alexa Fluor 633–WGA). Right, trajectories at left, presented with sinus boundaries outlined in gray. Scale bar, 20 μm.

duct lymph is inhibited within 1 h of drug administration[2]. This was much faster than expected for catabolism and subsequent resynthesis of $S1P_1$ receptors; for example, downregulation of epitope-tagged receptors requires exposure to FTY720 for several hours[5,14]. Moreover, FTY720 and its chiral analog AAL-(R) produce lymphocyte sequestration at subnanomolar free concentrations[15] that do not cause sufficient occupancy of the closely related $S1P_3$ receptor to induce cardiac arrhythmias[3,16], suggesting that lymphopenia results from an agonist action in the steep agonist binding range of $S1P_1$ receptors.

Finally, we found that $S1P_1$ antagonists W123 and VPC23019 reversed the inhibition of T cell motility and transendothelial migration caused by SEW2871, although they were without effect when applied alone. These data are especially difficult to reconcile with the hypothesis that lymphopenia results from receptor desensitization or downregulation, which would require that selective high-affinity antagonists mimic the action of SEW2871 in sequestering lymphocytes in the node. In contrast to that, we conclude that

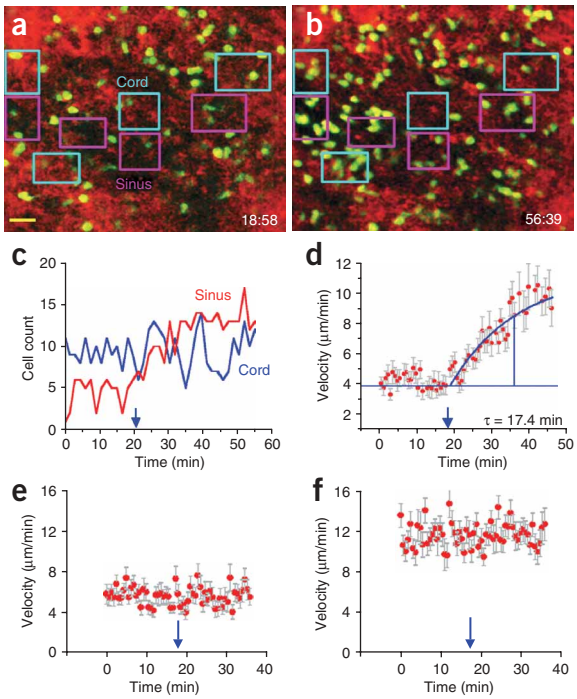

Figure 6 Rapid reversal of SEW2871 action by superfusion with the selective $S1P_1$ antagonist W123. (**a**) Two-photon image (maximum intensity projection through a 10-μm axial depth) of the medullary region at a single time point during superfusion with 5 μM SEW2871. Boxes indicate defined regions of comparable volumes in the sinus (magenta) and adjacent medullary cord (cyan) used to measure the cell numbers plotted in **c**. (**b**) Image of the same region of the node in **a** in the continued presence of SEW2871, captured 36 min after the addition of 20 μM W123 to the superfusion medium. Times of image acquisition in **a**,**b** are indicated in minutes:seconds; scale bar, 20 μm. (**c**) Average numbers of T cells in sinus (red) and medullary (blue) regions throughout a 54-minute imaging period. SEW2871 (5 μM) was present throughout, and W123 (20 μM) was added to the superfusate beginning at the time indicated by the downward arrow. (**d**) Recovery of T cell velocity after the addition of W123 (downward arrow) to SEW2871-containing medium. Data represent mean instantaneous velocities of 50 T cells and are representative of three experiments for each antagonist (**Supplementary Video 9** online). (**e**,**f**) The motility of T cells in the medulla (axillary node; **e**) and cortex (inguinal node; **f**) is unchanged by W123. Data show mean instantaneous velocities of 50 T cells in each region, measured in control nodes never exposed to SEW2871. Superfusion with W123 (20 μM) began where indicated by the downward arrows.

$S1P_1$-dependent nodal sequestration involves obligate agonism, not functional antagonism, and that the agonist signal is weak or absent during constitutive lymphocyte trafficking. Furthermore, we predict that $S1P_1$ receptor antagonists can reverse the lymphopenia induced by agonists such as SEW2871.

Where then do $S1P_1$ agonists act to regulate lymphocyte egress from the node? We favor the hypothesis[2] that SEW2871 and related immunosuppressants inhibit diapedesis across the endothelial barrier by acting on stromal gates that are constitutively open, but close in response to signaling events mediated by $S1P_1$ receptors on sinus endothelial cells, perhaps in concert with intrinsic changes in T cell function. The idea of a regulated physical barrier is supported most directly by our observations that T cells fail to traverse the stromal barrier in the presence of SEW2871 despite retaining motility in all other directions and that washout of the drug resulted in the restoration of bidirectional crossing at 'portals'. Consistent with that interpretation, FTY720 is known to have effect on endothelial cells, such as increasing tight-junction formation[17–19], and S1P has been documented to have key physiological and pathophysiological roles in the regulation of barrier function both in endothelial and epithelial cells *in vivo*[20].

In contrast to the hypothesis of stromal gating, however, other evidence points to an intrinsic T cell regulation by $S1P_1$ receptors[5,6]. Indeed, it is likely that both mechanisms may have mutually supportive functions[21]. In that context, the slowing of medullary T cell velocities by SEW2871 may be attributable to a direct action on the lymphocytes themselves, as suggested by the rapid effect of antagonist W123 on medullary T cell motility in the presence of agonist inhibition. In contrast, the dependence of T cell motility on local microenvironment and the lack of effect of SEW2871 and FTY720 (ref. 12) on T cell velocities in cortical zones[12] suggest an alternative explanation by which the slowing induced by $S1P_1$ agonists arises secondarily through changes in the external milieu through which T cells move. That is, reduction in T cell velocity might occur simply as a consequence of the high density of log-jammed T cells in the medulla or as a result of narrowing of the stromal gates.

Genetic studies involving $S1P_1$-null B cells and T cells have been extrapolated to suggest that immunosuppressants such as FTY induce lymphopenia through downregulation of $S1P_1$ receptors on lymphocytes[5,6]. Also, cyclical regulation of lymphocyte $S1P_1$ has been postulated as a mechanism for lymphocyte regulation in lymphoid organs despite the failure to show receptor surface expression on B cells that are readily sequestered by $S1P_1$ agonists[22]. Moreover, $S1P_1$ receptors are involved not only in controlling lymphocyte egress from lymph nodes but also in regulating their homing to the node through integrin activation[12].

Chemical and genetic studies of $S1P_1$ receptor modulation therefore do not directly correlate in two ways. First, $S1P_1$-null B cells and T cells show phenotypic abnormalities, with upregulation of CD69 (ref. 5), whereas long-term administration of both FTY720 (refs. 15,23) and SEW2871 (C. Alfonso, M. McHeyzer-Williams and H. Rosen, unpublished data) inhibits thymic egress while accelerating the shedding of CD69 on medullary single-positive thymocytes. Second, the rapidly reversible inhibition by S1P and related agonists[2] of T cell migration across the lymphatic endothelium and its restoration in the continuous presence of agonist by a molar excess of competitive antagonist do not support the idea of a mechanism of medullary egress control requiring $S1P_1$ receptor desensitization, degradation or deletion. Improved genetic tools capable of perturbing lymphocyte function without producing developmental abnormalities of phenotype (such as an increase in CD69), together with potent and bioavailable receptor antagonists, should allow the separation of lymphocytic and stromal contributions to the inducible and rapidly reversible control of lymphocyte egress *in vivo*.

In summary, our results have provided visualization of transendothelial migration of T cells into the lymphatic sinus, an important control point for lymphocyte egress from lymphoid organs. These results indicate obligate agonism of $S1P_1$ receptors in inhibition of lymphocyte egress through stromal portals. Our findings elucidate one of the basic mechanisms that regulate lymphocyte trafficking through and retention in the lymph node and may guide the development of improved therapeutic strategies for immunosuppression based on lipid modulators of egress control.

METHODS

$S1P_1$-selective agonist and antagonist. We used SEW2871 as a reversible, $S1P_1$-selective agonist[3,10] and W123 (3-{[(3-hexyl-phenylcarbamoyl)-methyl]-amino}-propionic acid) and VPC23019 ((*R*)-phosphoric acid mono-[2-amino-2-(3-octyl-phenylcarbamoyl)-ethyl] ester) as competitive antagonists. W123 antagonizes receptor activation by SEW2871 in both receptor-proximal assays such as GTPγS activation and receptor-distal responses such as mitogen-activated protein kinase activation (**Supplementary Fig. 3** online). VPC23019 was synthesized as described[11] and was characterized by mass spectrometry and nuclear magnetic resonance.

Adoptive transfer and induction of lymphopenia. Cells were isolated from spleens and lymph nodes of BALB/c mice (Jackson Laboratories) and were purified by magnetic negative selection with a $CD4^+$ T cell isolation kit (Miltenyi). $CD4^+$ T cells were labeled for 30–45 min at 37 °C with 4 μM 5-(and-6)-carboxyfluorescein diacetate, succinimidyl ester (Molecular Probes), followed by adoptive transfer of 10×10^6 to 15×10^6 cells by tail vein injection into each 4- to 6-week-old BALB/c recipient. After the cells equilibrated (about 12 h) between the blood and lymphoid compartments, and 4 h before collection of lymph nodes, lymphopenia was induced by gavage with 10 mg/kg of SEW2871 (in 10% DMSO and 25% Tween 20) or with vehicle alone[3].

Preparation of lymph nodes and fluorescent labeling of medullary structure. Peripheral and mesenteric lymph nodes were removed after CO_2 asphyxiation of mice and were stained with a fluorescence-labeled lectin for visualization of internal structures by two-photon imaging. Explanted nodes were soaked for 2–5 h on ice in RPMI medium containing 0.1 mg/ml of WGA conjugated to Alexa Fluor 633 (Molecular Probes) before two-photon imaging. SEW2871 (5 μM) was included in the incubation solution for nodes obtained from mice previously gavaged with the drug. We did two-photon and confocal microscopy on cervical, axillary and inguinal nodes and did not find appreciable differences between these nodes. Confocal images of paraformaldehyde-fixed, paraffin-embedded lymph node sections (**Fig. 1b–e**) were obtained as described[20]. In this case, intact nodes were first incubated with Alexa Fluor 633–WGA, and sections were then stained with rabbit antibody to mouse LYVE-1 for labeling of hyaluronan receptors on lymphatic endothelium and antibody to B220 (E-Bioscience) for labeling of B lymphocytes.

Two-photon imaging and analysis. Multidimensional (*x*, *y* and *z* axes, time and emission wavelength) two-photon microscopy was done as described[9] with femtosecond-pulsed excitation at 780 nm. Fluorescence emission was split by a 590-nm dichroic mirror into two detector channels and was used simultaneously to visualize structures stained with Alexa Fluor 633–WGA (red) and adoptively transferred T cells labeled with 5-(and-6)-carboxyfluorescein diacetate, succinimidyl ester (green). For imaging in the medullary region, lymph nodes were oriented with the hilum facing the dipping objective (Olympus 20×; numerical aperture, 0.9) of the upright microscope; otherwise, nodes were oriented with the hilum away from the objective for imaging of the T cell zone[9]. The node was maintained at 36 °C and was bathed with a continuous flow (superfusion) of RPMI medium 'bubbled' with carbogen (95% O_2 and 5% CO_2). SEW2871 (5 μM) was included in the medium for most nodes undergoing experimentation obtained from drug-treated mice. Washout of SEW2871 by RPMI medium or by the addition of 20 μM W123 or 10 μM VPC23019 to

the perfusion medium was used to effect recovery of lymphocyte migration across the lymphatic endothelium. Imaging volumes of 50-μm depth, with a *z*-axis resolution of 2.5 μm per step, were acquired at 17.4-second intervals with MetaMorph software (Universal Imaging). For more clear delineation of sinus boundaries, final images were formed by the construction of maximum intensity projections through 10-μm 'slices' in the *z*-axis (a projection through four adjacent *z*-planes, comparable in thickness to about 1.5 T cell diameters). The resultant video stack was corrected for axial drift that may occur during recordings to ensure that cell movement across the red-stained sinus represented a traversal of sinus barrier rather than movement above or under the sinus. To reduce selection bias in our analysis of motility and trajectory, 50–100 random T cells (regardless of location relative to sinuses, unless indicated otherwise) were tracked for each video segment to account for most of the distinctly visible cells.

Note: Supplementary information is available on the Nature Immunology website.

ACKNOWLEDGMENTS

We thank O. Safrina for some T cell isolation procedures; L. Forrest for guidance on animal handling; M. Peterson for lymph node immunohistology; X. Duong-Polk for the GTPγS assays; W. Cheng for VPC23019; and D. Jackson (University of Oxford, Oxford, UK) for the gift of LYVE-1. Supported by the National Institutes of Health (GM-41514 to M.D.C., GM-48071 to I.P., and AI-55509 and MH074404-01 to H.R.).

COMPETING INTERESTS STATEMENT

The authors declare that they have no competing financial interests.

Published online at http://www.nature.com/natureimmunology/
Reprints and permissions information is available online at http://npg.nature.com/reprintsandpermissions/

1. Brinkmann, V. FTY720: mechanism of action and potential benefit in organ transplantation. *Yonsei Med. J.* **45**, 991–997 (2004).
2. Mandala, S. *et al.* Alteration of lymphocyte trafficking by sphingosine-1-phosphate receptor agonists. *Science* **296**, 346–349 (2002).
3. Sanna, M.G. *et al.* Sphingosine 1-phosphate (S1P) receptor subtypes $S1P_1$ and $S1P_3$, respectively, regulate lymphocyte recirculation and heart rate. *J. Biol. Chem.* **279**, 13839–13848 (2004).
4. Rosen, H., Sanna, G. & Alfonso, C. Egress: a receptor-regulated step in lymphocyte trafficking. *Immunol. Rev.* **195**, 160–177 (2003).
5. Matloubian, M. *et al.* Lymphocyte egress from thymus and peripheral lymphoid organs is dependent on S1P receptor 1. *Nature* **427**, 355–360 (2004).
6. Allende, M.L., Dreier, J.L., Mandala, S. & Proia, R.L. Expression of the sphingosine 1-phosphate receptor, $S1P_1$, on T-cells controls thymic emigration. *J. Biol. Chem.* **279**, 15396–15401 (2004).
7. Cinamon, G. *et al.* Sphingosine 1-phosphate receptor 1 promotes B cell localization in the splenic marginal zone. *Nat. Immunol.* **5**, 713–720 (2004).
8. Miller, M.J., Wei, S.H., Cahalan, M.D. & Parker, I. Autonomous T cell trafficking examined in vivo with intravital two-photon microscopy. *Proc. Natl. Acad. Sci. USA* **100**, 2604–2609 (2003).
9. Miller, M.J., Wei, S.H., Parker, I. & Cahalan, M.D. Two-photon imaging of lymphocyte motility and antigen response in intact lymph node. *Science* **296**, 1869–1873 (2002).
10. Jo, E. *et al.* $S1P_1$-selective in vivo-active agonist from high throughput screening: Off-the-shelf chemical probes of receptor interactions, signaling and fate. *Chem. Biol.* **12**, 703–715 (2005).
11. Davis, M.D., Clemens, J.J., Macdonald, T.L. & Lynch, K.R. Sphingosine 1-phosphate analogs as receptor antagonists. *J. Biol. Chem.* **280**, 9833–9841 (2005).
12. Halin, C. *et al.* The S1P-analog FTY720 differentially modulates T cell homing via HEV: T cell-expressed $S1P_1$ amplifies integrin activation in peripheral lymph nodes but not in Peyer's patches. *Blood* **106**, 1314–1322 (2005).
13. Cyster, J.G. Chemokines, sphingosine-1-phosphate, and cell migration in secondary lymphoid organs. *Annu. Rev. Immunol.* **23**, 127–159 (2005).
14. Graler, M.H. & Goetzl, E.J. The immunosuppressant FTY720 down-regulates sphingosine 1-phosphate G-protein-coupled receptors. *FASEB J.* **18**, 551–553 (2004).
15. Rosen, H., Alfonso, C., Surh, C.D. & McHeyzer-Williams, M.G. Rapid induction of medullary thymocyte phenotypic maturation and egress inhibition by nanomolar sphingosine 1-phosphate receptor agonist. *Proc. Natl. Acad. Sci. USA* **100**, 10907–10912 (2003).
16. Forrest, M. *et al.* Immune cell regulation and cardiovascular effects of sphingosine 1-phosphate receptor agonists in rodents are mediated via distinct receptor subtypes. *J. Pharmacol. Exp. Ther.* **309**, 758–768 (2004).
17. Brinkmann, V., Cyster, J.G. & Hla, T. FTY720: sphingosine 1-phosphate receptor-1 in the control of lymphocyte egress and endothelial barrier function. *Am. J. Transplant.* **4**, 1019–1025 (2004).
18. Sanchez, T. *et al.* Phosphorylation and action of the immunomodulator FTY720 inhibits vascular endothelial cell growth factor-induced vascular permeability. *J. Biol. Chem.* **278**, 47281–47290 (2003).
19. Peng, X. *et al.* Protective effects of sphingosine 1-phosphate in murine endotoxin-induced inflammatory lung injury. *Am. J. Respir. Crit. Care Med.* **169**, 1245–1251 (2004).
20. Gon, Y. *et al.* : $S1P_3$ receptor-induced loss of epithelial tight junctions compromises lung barrier integrity. *Proc. Natl. Acad. Sci. USA* **102**, 9270–9275 (2005).
21. Rosen, H. & Goetzl, E.J. Sphingosine 1-phosphate and its receptors: an autocrine and paracrine network. *Nat. Rev. Immunol.* **5**, 560–570 (2005).
22. Lo, C.G., Xu, Y., Proia, R.L. & Cyster, J.G. Cyclical modulation of sphingosine-1-phosphate receptor 1 surface expression during lymphocyte recirculation and relationship to lymphoid organ transit. *J. Exp. Med.* **201**, 291–301 (2005).
23. Yagi, H. *et al.* Immunosuppressant FTY720 inhibits thymocyte emigration. *Eur. J. Immunol.* **30**, 1435–1444 (2000).